Mon. Not. R. Astron. Soc. **000**, 1–10 (2007) Printed 2 February 2008 (MN LATEX style file v2.2)

Analytical Approach to Subhaloes Population in Dark Matter Haloes

Carlo Giocoli[1], Lidia Pieri[2,3] and Giuseppe Tormen [1]
*

[1] Dipartimento di Astronomia, Università degli Studi di Padova, Vicolo dell'osservatorio 2 I-35122 Padova, Italy
[2] Istituto Nazionale di Astrofisica - Osservatorio Astronomico di Padova, Vicolo dell'osservatorio 2 I-35122 Padova, Italy
[3] Istituto Nazionale di Fisica Nucleare - Sezione di Padova, Via Marzolo 8 I-35131 Padova, Italy

ABSTRACT

In the standard model of cosmic structure formation, dark matter haloes form by gravitational instability. The process is hierarchical: smaller systems collapse earlier, and later merge to form larger haloes. The galaxy clusters, hosted by the largest dark matter haloes, are at the top of this hierarchy representing the largest as well as the last structures formed in the universe, while the smaller and first haloes are those Earth-sized dark subhaloes which have been both predicted by theoretical considerations and found in numerical simulations, though it does not exist any observational hints of their existence. The probability that a halo of mass m at redshift z will be part of a larger halo of mass M at the present time can be described in the frame of the extended Press & Schecter theory making use of the progenitor (conditional) mass function. Using the progenitor mass function we calculate analytically, at redshift zero, the distribution of subhaloes in mass, formation epoch and rarity of the peak of the density field at the formation epoch. That is done for a Milky Way-size system, assuming both a spherical and an ellipsoidal collapse model. Our calculation assumes that small progenitors do not lose mass due to dynamical processes after entering the parent halo, and that they do not interact with other subhaloes. For a ΛCDM power spectrum we obtain a subhalo mass function $\mathrm{d}n/\mathrm{d}m$ proportional to $m^{-\alpha}$ with a model-independent $\alpha \sim 2$. Assuming the dark matter is a weakly interacting massive particle, the inferred distributions is used to test the feasibility of an indirect detection in the γ-rays energy band of such a population of subhaloes with a GLAST-like satellite.

Key words: galaxies: halo - cosmology: theory - dark matter - methods: analytical

1 INTRODUCTION

The present-day description of the universe includes the presence of a large amount of cold dark matter (CDM) whose nature and distribution is unknown. This Dark Matter (DM) provides about 26 % of the energy budget of the universe.

The amount and properties of CDM is well constrained by astrophysical observations such as the anisotropies in the Cosmic Microwave Background, large scale structure and distant type I A supernovae (Spergel et al. 2003; Astier et al. 2006; Tegmark et al. 2006). On the other hand, two main open questions arise. The first concerns the particle physics nature of the CDM. Weakly interacting massive particles (WIMPs) are attractive candidates since their relic abundance can fit the observed one (Dimopoulos 1990). Stable neutralinos in supersymmetric extensions of the standard model (SUSY) (Jungman et al. 1996; Bertone et al. 2005a) or Kaluza-Klein particles (KKP) in theories with a TeV^{-1} size universal extra dimension (Appelquist et al. 2001; Servant & Tait 2003) are the most commonly studied particles. Since these particles have never been observed, there is a large uncertainty on the prediction of their effects which has to be taken into account. The other open question regards the distribution of DM inside the haloes. Numerical N-body simulations (Navarro et al. 1997; Diemand et al. 2004c; Navarro et al. 2003), whose scale resolution is about $\sim 0.1\,\mathrm{kpc}$, allow solely an extrapolation of the very inner slope of the DM profile and do not take into account interactions with the baryons which fall in the DM potential well or the presence of inner cores (Berezinsky et al. 2003) or the controverse effect of the presence of a black hole at the centre of the halo (Ullio et al. 2001; Bertone et al. 2005b; Bertone & Merritt 2005; Merritt et al. 2002). Experimental data on DM distribution in the haloes of galaxies and clusters are not conclusive too (see, i.g., the discus-

* Email: carlo.giocoli@unipd.it, lidia.pieri@oapd.inaf.it, giuseppe.tormen@unipd.it.

sion in Fornengo et al. (2004)). In the hierarchical formation scheme of the CDM scenario, large systems are the result of the merging and accretion of smaller haloes (subhaloes), whose dense central cores would survive the merging event and continue to orbit within the parent halo, as shown by high resolution N-body simulations (Moore et al. 1999; Ghigna et al. 2000; Blasi & Sheth 2000). CDM models are characterized by an excess of power on small scales. The arising divergence of the linear density constrast at large wavenumbers has been proved to be damped by collisional processes and free streaming, respectively before and after kinetic decoupling, leading to exponential damping of the linear CDM density contrast and to the existence of a typical scale (Jeans scale) for the first haloes corresponding to a Jeans mass about $10^{-6} M_{\odot}$ (Hofmann et al. 2001; Green et al. 2004, 2005). Numerical simulations have indeed reproduced hierarchical clustering in CDM cosmologies with a mass resolution sufficient to resolve the Jeans mass (Diemand et al. 2005a) with particle mass $m_p = 1.2 \times 10^{-10}\, M_{\odot}$ and force resolution of $\epsilon = 0.01$ pc; however such a high resolution run could be evolved only to $z = 26$, in a very small spatial patch, and producing haloes of mass $[10^{-6}, 10^{-4}]\, M_{\odot}$.

Among the simulations evolved on larger scales and to redshift $z = 0$, present milestones are the Millennium Simulation (Springel et al. 2005) and the Via Lactea Simulation (Diemand et al. 2007a). The first is a cosmological N-Body run with over 10 billion particles in a cubic region 500 Mpc/h on a side (particle mass $m_p = 1.23 \times 10^9 M_{\odot}$; force resolution $\epsilon = 7$ kpc); the second was done to obtain a simulated Milky Way with the highest possible mass resolution (particle mass $m_p = 2.09 \times 10^3 M_{\odot}$; force resolution $\epsilon = 90$ pc). However a simulation with the mass and force resolution similar to that of (Diemand et al. 2005a), evolved to redshift zero over a region containing a mass comparable to that of our Galaxy would require about 10^{20} particles and a time resolution of a few years. Such requirements are way beyond the computational capabilities of present-day supercomputers: applying Moore's law and starting from present day state-of-the-art, a run like this could be performed in roughly 50 years from now.

A reasonable alternative is to study the clustering properties of Milky Way-like systems through an analytical approach. We use the fact that the probability that a halo of mass m at redshift z will be part of a larger halo of mass M at the present time is described by the progenitor conditional mass function $f(m, z|M, z_0 = 0)$, according to the so-called extended Press & Schechter theory. Using the progenitor mass function, we can calculate analytically, at redshift zero, the distribution of subhaloes in mass, formation epoch and rarity of the peak of the density field at the formation epoch. That is done for a Milky Way-size system, assuming both a spherical and an ellipsoidal collapse model.

Numerical simulations described in Diemand et al. (2005b) show that the distribution of material originating from the earliest branches of the merger tree within the present day haloes depends on the σ-peaks of the primordial density fluctuation field it belonged to. We extend their numerical results by performing an analytical estimate of the density peaks distribution as a function of the halo mass traced back to the smallest scale haloes, thus avoiding the limitation imposed by numerical simulations. In this way we obtain a realistic estimate of the distribution and mass function of the whole population of subhaloes.

Such an analytical estimate can provide a powerful tool to take into account the effect of early high-density peaks in present day haloes.

This is particularly important in the framework of dark matter indirect detection, since a high σ-peak halo translates into a higher concentration and thus a higher value for the density squared which has to be integrated along the line of sight to obtain a prediction for particle fluxes coming from dark matter annihilation.

Given some model for the hierarchical formation of our Galaxy, and for the internal structure of subhaloes, DM may be in fact indirectly detected using annihilation rates predicted from particle physics (Bergström 2000; Bertone et al. 2005a) through the observation of high density point-source or extended regions inside our Galaxy. If we restrict ourselves to γ-ray observations, these can be obtained using either atmospheric Cerenkov telescopes (Weekes et al. 1997; Aharonian et al. 1997; Baixeras 2003) or satellite-borne detectors like GLAST (Morselli et al. 1997). The detectability of DM substructures with GLAST has been widely discussed in the literature (see, e.g. Pieri et al. (2007) and references therein). The small mass haloes have been found to give the main contribution to an unresolved γ-ray foreground arising from DM annihilation, while their detection as resolved objects has been proved to be very unlike. Indeed the unresolved subhalo foreground is prominent above the MW smooth foreground far from the Galactic Center, where the overall flux is still too low to be detected.

In this paper we apply the analytical derivation of the subhalo population properties, such as the σ-peak distribution, on the indirect detection of γ-rays. We thus study the possibility that high σ-peak material could arise the foreground level above the detectability threshold of a GLAST-like large field of view satellite.

As in Pieri et al. (2007), we use different models for the virial concentration of subhaloes.

The paper is organized as follows: in Sec. 2, we review the spherical and ellipsoidal collapse model and their properties. In Sec. 3 we describe the original analytical derivation of the density peak distribution as function of the halo mass, and the subhaloes mass function for a present day halo with mass $M = 10^{12}\, M_{\odot}/h$. In Sec. 4 we estimate the upper bound for the contribution to the γ-ray flux due to the presence of a population of subhaloes inside the Milky Way. In Sec. 5, we study the prospects for detection of substructures with a GLAST-like experiments in our best case scenario. A discussion of our results can be found in Sec. 6.

2 EXTENDED-PRESS & SCHECHTER: FROM PROGENITORS TO SUBHALOES

In the hierarchical picture of galaxy formation, structures up to protogalactic scale grow as a consequence of repeated merging events. Smaller systems collapse at high redshifts, when the universe is denser, and subsequently assemble to form bigger and bigger haloes (Lacey & Cole 1993). This merging history is often represented by the so called "merger-trees".

Smaller systems accreted onto a larger halo along its

merging-history-tree and still surviving at a later time are called "substructures" or "subhaloes" (Ghigna et al. 1998; Tormen et al. 2004; Gao et al. 2004; De Lucia et al. 2004a; van den Bosch et al. 2005). In what follows we will discuss an analytical approach to derive the mass function of subhaloes. We will use the simplifying assumption that no tidal stripping nor merging events among substructures happen. In this approach the mass of each subhalo remains constant in time, and equals the original virial mass (Eke et al. 1996) of the progenitor halo at the considered redshift. A similar study was carried out by Sheth (2003), who calculated the subhalo mass function using the creation rate of the progenitors of a present day dark matter halo; our approach is different: we derive the subhalo mass function from the entire population of progenitors (as shown by Eq. 4), in order to allow a direct comparison with the N-Body results of Diemand et al. (2005b).

2.1 Conditional Mass Function

Let us consider a halo with virial mass M at some final redshift z_0. According to the hierarchical picture of galaxy formation, going backward in time the halo will be splitted in smaller and smaller systems, called "progenitors". Mass conservation tells us that the sum of all masses of progenitor haloes at any given redshift equals the mass of the halo at z_0. Let us define the conditional mass function $f(m, z|M, z_0)\mathrm{d}m$ as the fraction of mass belonging to haloes with mass between m and $m + \mathrm{d}m$ at redshift z, which are progenitors of a halo of mass M (a M-halo) at a later redshift z_0.

Assuming the spherical collapse model (Press & Schechter 1974), we can express m and z as a function of the new variables s and δ_{sc}. The conditional mass function is independent on the power spectrum of density fluctuations and it is described as (Lacey & Cole 1993):

$$f(s, \delta_{sc}|S, \delta_0)\mathrm{d}s = \frac{\delta_{sc} - \delta_0}{\sqrt{2\pi(s-S)}} \exp\left\{-\frac{(\delta_{sc}-\delta_0)^2}{2(s-S)}\right\}\frac{\mathrm{d}s}{s-S}, \tag{1}$$

where $s = \sigma^2(m)$ is the square of the mass variance of a m-halo, and δ_{sc} is the spherical collapse overdensity at redshift z. S and δ_0 are the mass variance of an M-halo and the spherical collapse overdensity at the present time, respectively. To compute the mass variance we have chosen a power spectrum with primordial spectral index $n = 1$, and a transfer function obtained from CMBFAST (Seljak & Zaldarriaga 1996) for a concordance ΛCDM universe (Ω_m, Ω_Λ, h = 0.3, 0.7, 0.7) with $\sigma_8 = 0.772$, extended down to a mass $M = 10^6 M_\odot/h$.

We have integrated this power spectrum using a top-hat filter in real space. To obtain the mass variance until the typical Jeans neutralino mass we linearly extrapolate the $\log(m)$-s relation to $M = 10^{-6} M_\odot/h$.

Over the last ten years N-Body simulations have shown that the collapse of dark matter haloes is actually not well described by an isolated spherical model; the influence of sourrounding proto-haloes can be reproduced using an ellipsoidal model (Sheth, Mo & Tormen 2001; Sheth & Tormen 2002).

In the excursion set approach, the progenitor mass function of a halo is described by the conditional probability of first upcrossing distribution. Such a probability is well fitted by a random walk in the plane (s, δ), starting from (S, δ_0) (Bond et al. 1991).

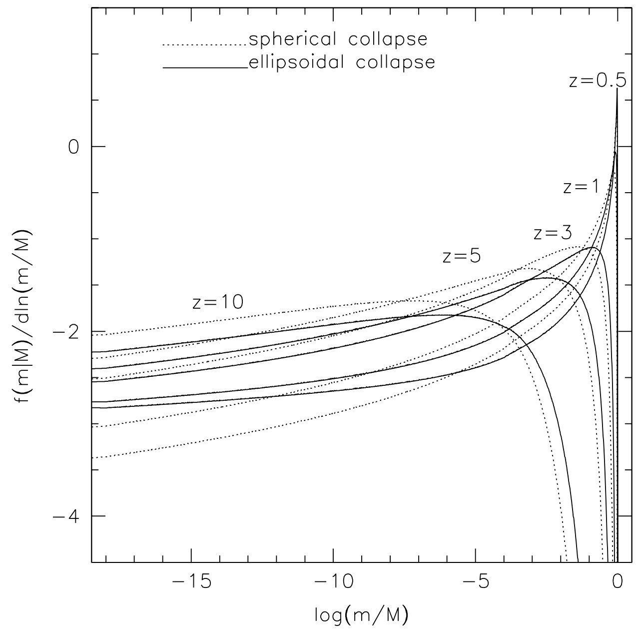

Figure 1. Ellipsoidal (solid) and spherical (dotted) conditional mass function computed for a present-day dark matter halo with mass $10^{12} M_\odot/h$ and for five different redshifts.

In the spherical collapse model this barrier has a constant height, defined by the collapse redshift: $B_{sc}(s, \delta_{sc}) = \delta_{sc}$. For the ellipsoidal collapse case the barrier height is not constant, but depends on s and on δ_{sc} as described by the following equation:

$$B_{ec}(s, \delta_{sc}) = \sqrt{q}\delta_{sc}\left[1 + \beta\left(\frac{s}{q\delta_{sc}^2}\right)^\gamma\right]. \tag{2}$$

Sheth, Mo & Tormen (2001) found $q = 0.707$, $\beta = 0.5$ and $\gamma = 0.6$; the value of the last two parameters is motivated by an analysis of the collapse of homogeneous ellipsoids, whereas the value of q comes from requiring that the predicted halo abundances match what is found in the simulations.

Considering the barrier described in Eq.2, Sheth & Tormen (2002) found an approximate solution for the diffusion equation, expressed as follows:

$$\begin{aligned} f(s, \delta_{sc}|S, \delta_0)\mathrm{d}s &= \frac{|T(s, \delta_{sc}|S, \delta_0)|}{\sqrt{2\pi(s-S)}} \times \qquad (3) \\ &\exp\left\{-\frac{[B(s,\delta_{sc}) - B(S,\delta_0)]^2}{2(s-S)}\right\}\frac{\mathrm{d}s}{s-S}, \end{aligned}$$

with $T(s|S)$:

$$T(s, \delta_{sc}|S, \delta_0) = \sum_{n=0}^{5} \frac{(S-s)^n}{n!} \frac{\partial^n[B(s,\delta_{sc}) - B(S,\delta_0)]}{\partial s^n}.$$

In Figure 1 we show the conditional mass function at five different redshifts for a halo with present-day mass $M = 10^{12} M_\odot/h$, both for the spherical (dotted curves) and ellipsoidal (solid) collapse prediction. It can be observed that the halo is splitted in smaller and smaller progenitors at

higher redshifts; discrepancies between the two models depend both on mass and on redshift.

Comparing the two prediction at fixed redshift, one can note that the spherical model predicts more progenitors at intermediate mass, and fewer at both very small and very large masses, compared to the ellipsoidal model (Sheth & Tormen 2002). In other words, the two predictions cross each others in two points, although these crossings do not necessarily fall in the range of masses plotted in the Figure.

A direct consequence of this is that massive progenitors exist at higher redshifts in the ellipsoidal collapse, and the distribution of formation redshifts (defined as the earliest epoch when a halo assembles half of its final mass in one system) is consequently shifted to earlier epochs (Giocoli et al. 2007).

From $f(s, \delta_{sc}|S, \delta_0)\mathrm{d}s$ we can write the total number of progenitors at any given redshift as:

$$N(m, \delta_{sc}|M, \delta_0)\mathrm{d}m = \frac{M(S)}{m(s)} f(s, \delta_{sc}|S, \delta_0)\mathrm{d}s\,. \quad (4)$$

Considering a scale free power spectrum $P(k) \propto k^n$, the mass variance scales as $s(m) \propto m^{-(n+3)/3}$, and the number of progenitors can be explicitely written in terms of s:

$$N(m, \delta_{sc}|M, \delta_0)\mathrm{d}m = \left(\frac{s}{S}\right)^{(n+3)/3} f(s, \delta_{sc}|S, \delta_0)\mathrm{d}s\,. \quad (5)$$

2.2 Number of progenitors

Interating Eq. 4 over mass we obtain the total number of progenitors in the given mass interval, as a function of redshifts:

$$\mathrm{d}n(z, \Delta m) = \int_{m_i}^{m_f} N(m, \delta_{sc}|M, \delta_0)\mathrm{d}m = \mathbb{N}(z)\Big|_{m_i}^{m_f}\,, \quad (6)$$

where m_i and m_f represent the bounds of the interval. For a white-noise power spectrum (scale free with $n = 0$) and a spherical collapse mass function, a primitive of this integral can be written as:

$$\mathbb{N}(z) = \frac{1}{S\sqrt{2\pi}}\left\{ \mathrm{e}^{-\frac{(\delta_{sc}-\delta_0)^2}{2(s-S)}} \left[2\sqrt{s-S}(\delta_{sc}-\delta_0) - \mathrm{e}^{\frac{(\delta_{sc}-\delta_0)^2}{2(s-S)}} \sqrt{2\pi}[S-(\delta_{sc}-\delta_0)^2]\mathrm{erf}\left(\frac{\delta_{sc}-\delta_0}{\sqrt{2(s-S)}}\right)\right]\right\}. \quad (7)$$

In Figure 2 we show the total number of progenitors in five different mass decades, for a halo with mass $M = 10^{12} M_\odot/h$ at z_0, as a function of redshifts. We have assumed a concordance ΛCDM power spectrum and have integrated Eq. 4 numerically. The solid lines represent the prediction for the ellipsoidal collapse model while the solid ones refer to the ellipsoidal model. From top to bottom the curves represent the following mass bins: $[h\,10^{-6}, 10^{-5}]$, $[10^{-1}, 1]$, $[10^2, 10^3]$, $[10^6, 10^7]$ and $[10^9, 10^{10}]$, all but the first expressed in term of $M_\odot/h$.

It can be observed that the spherical collapse, for a fixed mass bin, underpredicts the number of haloes at high redshifts compared to the ellipsoidal model. We will see in the next sections that if we consider the variable $\nu(z, m) = \delta_{sc}(z)/\sigma(m)$, for any given mass this will result in the inequality $\nu_{ec}(m) > \nu_{sc}(m)$.

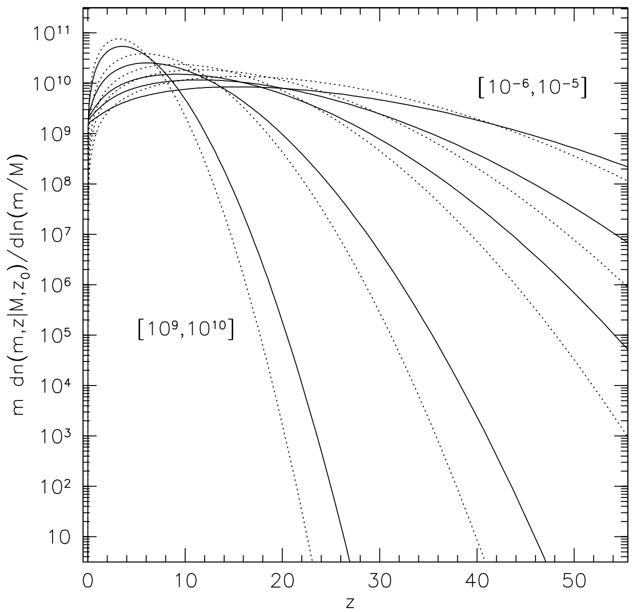

Figure 2. Total number of progenitors in a given mass bin, as a function of redshifts, for a present day halo with mass $M = 10^{12}\,M_\odot/h$. For each mass bin we show the prediction for spherical (dotted lines) and ellipsoidal (solid) collapse models.

3 UNEVOLVED SUBHALOES MASS FUNCTION FROM THE MERGER TREE OF A PARENT M-HALO

The progenitors mass function, integrated over δ_{sc}, gives the total number of progenitors of mass between m and $m+\mathrm{d}m$ that a halo of final mass M has had at all times:

$$\frac{\mathrm{d}n(m)}{\mathrm{d}m} = \int_{\delta_0}^{\infty} \frac{M}{m} f(s, \delta_{sc}|S, \delta_0)\mathrm{d}\delta_{sc}\,; \quad (8)$$

in the case of the spherical collapse this integral results in:

$$\frac{\mathrm{d}n(m)}{\mathrm{d}\ln(m)} = \frac{M}{\sqrt{2\pi}} \frac{|\mathrm{d}s/\mathrm{d}m|}{\sqrt{s-S}} \propto m^{-\alpha}\,, \quad (9)$$

with $\alpha \approx 1$ for a LCDM power spectrum. Since the same system may be a progenitor of the same final halo at more than one redshift, integrating the progenitor mass function overcounts the total number of progenitors. The result of this integration must then be properly re-normalized by imposing the constrain coming from (Diemand et al. 2005a) that roughly 10% of the total Milky Way mass ($M = 10^{12} M_\odot/h$) is in systems with mass ranging from 10^7 to $10^{10}\,M_\odot/h$:

$$\int_{10^{-5}}^{10^{-2}} \frac{m}{M}\mathrm{d}n = 0.1 \quad (10)$$

In Figure 3 we plot the differential mass distribution of subhaloes in a $10^{12}\,M_\odot/h$ (Milky Way-like) dark matter

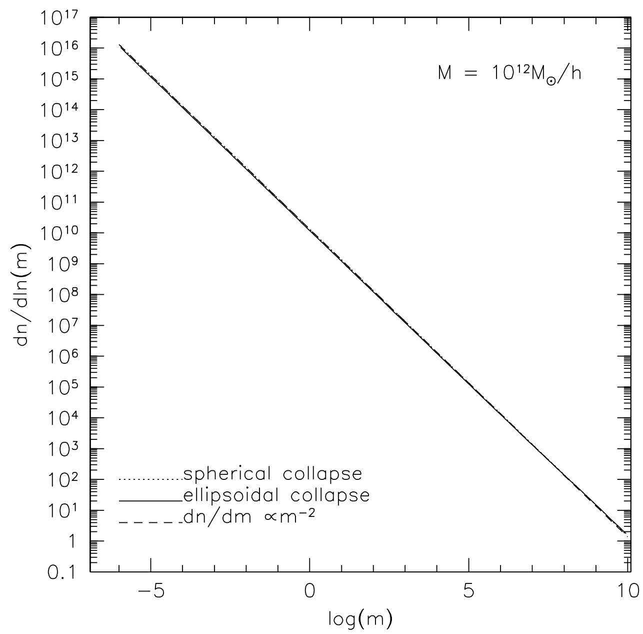

Figure 3. Differential distribution of subhaloes in a $10^{12}\,M_{\odot}/h$ dark matter halo. The distribution has a slope approximatively equal to 1 and has been normalized considering that 10% of the total mass is in subhaloes with mass from 10^7 to $10^{10}\,M_{\odot}/h$.

halo. The distribution has a power law behaviour approximately described by the relation:

$$\frac{\mathrm{d}n(m)}{\mathrm{d}m} = Am^{-\gamma}\,, \tag{11}$$

with $\gamma \approx 2$ for both the spherical and the ellipsoidal collapse model, respectively[1]. Once fixed the normalization factor, we find that the differential distribution of the subhaloes is independent on the mass of the progenitor halo, M, considering all the progenitors with mass from $10^{-6}\,M_{\odot}$ to $m/M = 0.01$.

3.1 Progenitors σ-peak in the host halo

Using high resolution N-Body simulations, Diemand et al. (2005b) studied the spatial distribution - at $z = 0$ - of matter belonging to high redshift progenitors of a given system. They found that this distribution mainly depends on the rareness of the density peak corresponding to the progenitor, expressed in terms of $\nu = \delta_{sc}/\sigma(M, z)$, and is largely independent on the particular value of z and M: matter from high ν progenitors ends up at smaller distances from the center of the final system.

We can understand this in term of the revised secondary infall (Quinn & Zurek 1988; Zaroubi et al. 1996): the formation of haloes in N-Body simulations preserves ranking of particle binding energy, that is, particles in the cores of progenitor haloes will end up in the core of the final system. Equally, particles from progenitors accreted at earlier times, hence possessing more negative initial binding energies, will likely have a more negative final energy, and so be more centrally concentrated than average matter.

At fixed redshift (hence at fixed δ_{sc}), higher mass progenitors have a larger ν, are more self-bound than smaller mass ones, and thus end up closer to the center of the final system. Analogously, for a fixed progenitor mass, higher redshift progenitors have a larger δ_{sc}, hence a larger ν; since at higher redshift the universe is denser, they also are more self-bound than lower redshift siblings, and so end up closer to the center of final system.

In Figure 4 we plot the subhalo mass function in terms of ν. To compute the factor ν for each progenitor we integrated the total number of progenitors in a given mass bin (Eq. 6), at all redshifts. In the top panel we consider all the progenitors at all redshifts, with mass in the full range $h10^{-6}$ to $10^{10}\,M_{\odot}/h$; in the bottom panel we show the similar distribution only for the smallest and larger decade of the progenitors mass.

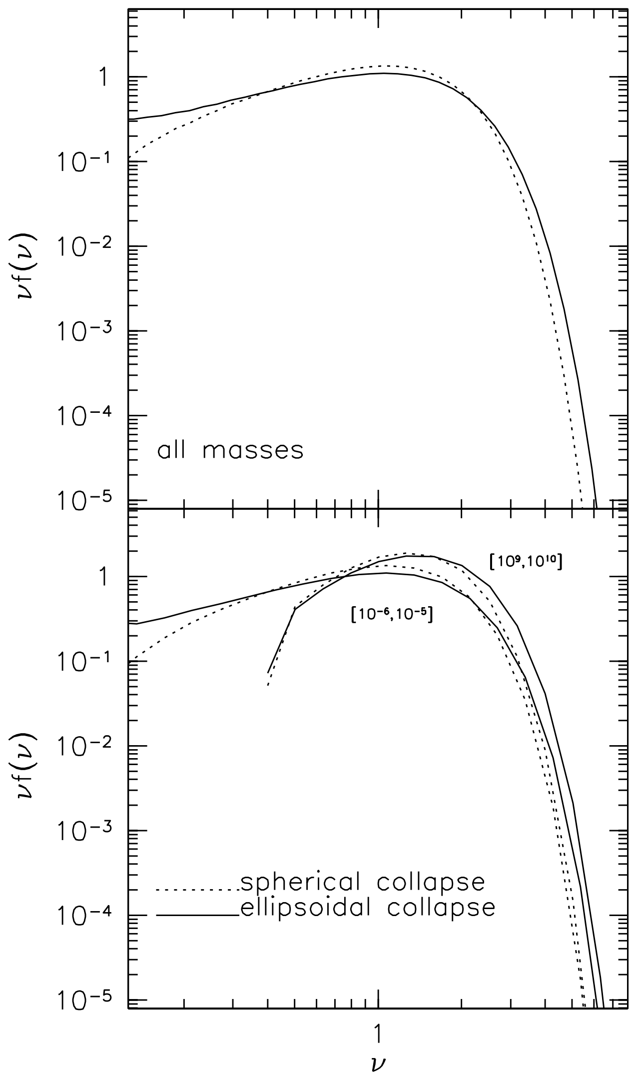

Figure 4. Progenitor mass function integrated over all redshifts. In the top panel we show the distribution for all the masses, while in the bottom panel we consider only progenitors in the first and last subhalo mass decades.

[1] A least-squares fit on the points gives $\gamma_{\rm sc} = -1.9972 \pm 0.0001$ and $\gamma_{\rm ec} = -1.9937 \pm 0.0003$.

4 γ-RAY FLUX FROM GALACTIC SUBSTRUCTURES

4.1 Modeling Galactic halo and substructures

We model the distribution of DM in our Galaxy after Diemand et al. (2005b).
For the smooth component of the Milky Way we use the best fit to the high resolution numerical experiments of Diemand et al. (2005a):

$$\rho_\chi(r) = \frac{\rho_s}{\left(\frac{r}{r_s}\right)^\gamma \left[1 + \left(\frac{r}{r_s}\right)^\alpha\right]^{(\beta-\gamma)/\alpha}} \tag{12}$$

with $(\gamma, \beta, \alpha) = (1.2, 3, 1)$. The scale radius r_s and density ρ_s, are constrained by the virial properties of the halo. Following Diemand et al. (2005b) we adopt $r_s = 26\,\mathrm{kpc}$, while ρ_s has to be normalized to the virial mass of the smooth DM halo. We include a physical cutff $r_{cut} = 10^{-8}\,\mathrm{kpc}$ which represents the distance at which the self-annihilation rate equals the dynamical time of spike formation.

We shape the spatial distribution of subhaloes according to the fact that it traces the mass distribution of the parent halo from r_{vir} down to a minimum radius $r_{min}(M)$ where tidal effects become important. We use Eq. 12 together with the fact that the dependence from the initial conditions when the haloes accreted onto the present-day Milky Way halo is set through the parameter $\nu(M)$. We then use the parametrization obtained in Diemand et al. (2005b):

$$r_s \longrightarrow r_\nu = f_\nu r_s$$

$$f_\nu = \exp(\nu/2)$$

$$\beta \longrightarrow \beta_\nu = 3 + 0.26\nu^{1.6} \tag{13}$$

This parametrization reflects the fact that material accreted in areas with high density fluctuations is more concentrated toward the centre of the galaxy, and has a steeper outer slope. We also use the mass function derived in Sec. 2 to model the number density of subhaloes per unit mass at a distance r from the GC, for a given $\nu(M)$:

$$\rho_{sh}(M, r, \nu) = \frac{AM^{-2}\theta(r - r_{min}(M))}{\left(\frac{r}{r_\nu(M)}\right)^\gamma \left[1 + \left(\frac{r}{r_\nu(M)}\right)^\alpha\right]^{(\beta_\nu-\gamma)/\alpha}}, \tag{14}$$

in units of $M_\odot^{-1}\,\mathrm{kpc}^{-3}$. The mass dependence in r_ν depends reflects the mass dependence of the virial parameter $r_s = r_{vir}/c_{vir}$. The effect of tidal disruption is taken into account through the step function $\theta(r - r_{min}(M))$, where $r_{min}(M)$ is estimated following the Roche criterion. A is a normalization factor obtained by imposing that 10% of the MW mass is distributed in subhaloes with masses in the range $10^7 - 10^{10} M_\odot$ (Diemand et al. 2005a) as in Sec.2.

As a result about 50% of the Milky Way mass is contained within $\sim 2 \times 10^{16}$ subhaloes in the mass range $[10^{-6}, 10^{10}] M_\odot$. The solar neighborhood density is $\sim 280\,\mathrm{pc}^{-3}$, mainly constituted by haloes with mass of $10^{-6} M_\odot$. The halo closest to the Earth is expected to be located $\sim 9.5 \times 10^{-2}$ pc away.

The remaining 50% of the Milky Way mass is assumed to be smoothly distributed, and we use this half mass value to normalize ρ_s in Eq. 12.

Few constraints exist on the density profile of each subhalo. Numerical simulations (Diemand et al. 2005a, 2006, 2007b) suggest they were formed with a NFW profile, which is described by Eq. 12 with $(\gamma, \beta, \alpha) = (1, 3, 2)$. Even if subhaloes probably underwent tidal stripping and consequent mass loss after merging, their higher central density should prevent the inner regions from being affected. Pieri et al. (2007) explored different possibilities for the concentration parameter $c_{vir} = r_{vir}/r_s$, where r_{vir} is defined as the radius at which the mean halo density is 200 times the critical density. Following their guidelines, we use two models for the concentration c_{vir}: we assume that the inner structure of subhaloes is either fixed at the time they merge onto the parent halo (z-labeled model) or that it evolves with redshift until the present time (0 model). In model $\mathrm{B}_{ref,0}$ the NFW concentration is computed at $z = 0$ according to Bullock et al. (2001) (hence the prefix B), and extrapolated to low masses. In model $\mathrm{B}_{ref,z}$, the values of $c_{vir}(M, z)$ are obtained from those at $z = 0$ using the evolutionary relation $c_{vir}(M, z) = c_{vir}(M, z = 0)/(1 + z)$, where the merging redshift z is determined by the knowledge of the value of ν assigned to each progenitor. Therefore, subhaloes are much denser in model $\mathrm{B}_{ref,z}$than in model $\mathrm{B}_{ref,0}$.

The values c_{vir} thus found refer to progenitors formed from average density fluctuations ($\nu = 1\sigma$ peaks of the fluctuation density field). However, haloes with equal mass at redshift z_1 may have assembled at different previous epochs; specifically, if we call $z_i > z_1$ the redshift of mass assembly for progenitors observed at redshift z_1, the amplitude of the initial density fluctuations producing the progenitors is an increasing function of z_i. Therefore, their concentration $c(M, z)$ is also an increasing function of the peak amplitude ν. To account for this effect, we use the relation $c_{vir}(M, \nu) = \nu(M) c_{vir}(M, \nu = 1)$, which has been tested against simulations by Diemand et al. (2005b).

4.2 Modeling the γ-ray flux from Dark Matter annihilation

We model the photon flux from neutralino annihilation in the population of galactic subhhaloes following Pieri et al. (2007). Given a direction of observation defined by the angle–of–view ψ from the Galactic Center, and a detector with angular resolution θ, the γ-ray flux can be parametrized as:

$$\frac{d\Phi_\gamma}{dE_\gamma}(E_\gamma, \psi, \theta) = \frac{d\Phi^{\mathrm{PP}}}{dE_\gamma}(E_\gamma) \times \Phi^{\mathrm{cosmo}}(\psi, \theta) \tag{15}$$

The particle physics dependence in Eq. 15 is given by the annihilation spectrum and DM properties and is embedded in the term:

$$\frac{d\Phi^{\mathrm{PP}}}{dE_\gamma}(E_\gamma) = \frac{1}{4\pi} \frac{\sigma_{\mathrm{ann}} v}{2m_\chi^2} \cdot \sum_f \frac{dN_\gamma^f}{dE_\gamma} B_f. \tag{16}$$

m_χ is the DM particle mass, $\sigma_{\mathrm{ann}} v$ is the self–annihilation cross–section times the relative velocity of the two annihilating particles, and dN_γ^f/dE_γ is the differential photon spectrum for a given final state f with branching ratio B_f, which we take from Fornengo et al. (2004).

The line–of–sight integral defined as:

$$\Phi^{\rm cosmo}(\psi,\Delta\Omega) = \int_M dM \int_\nu d\nu \int\int_{\Delta\Omega} d\theta d\phi \int_{\rm l.o.s} d\lambda \int_c dc$$

$$[\rho_{sh}(M, R(R_\odot,\lambda,\psi,\theta,\phi),\nu) \times P(\nu(M)) \times P(c(M)) \times$$

$$\times\, \Phi^{\rm cosmo}_{halo}(M, r(\lambda,\lambda',\psi,\theta',\phi'),\nu,c) \times J(x,y,z|\lambda,\theta,\phi)] \quad (17)$$

accounts for the influence of cosmology in the flux computation. $\Delta\Omega$ is the solid angle defined by the angular resolution of the instrument, $J(x,y,z|\lambda,\Delta\Omega)$ is the Jacobian determinant, $R = \sqrt{\lambda^2 + {R_\odot}^2 - 2\lambda R_\odot C}$, is the galactocentric distance and r is the radial distance inside the single subhalo. $R_\odot$ is the distance of the Sun from the galactic center and $C = \cos(\theta)\cos(\psi) - \cos(\phi)\sin(\theta)\sin(\psi)$. $P(\nu(M))$ is the probability distribution function for the peak rarity $\nu(M)$ calculated using the extended Press-Schechter formalism. $P(c(M))$ is the lognormal probability distribution for c centered on $c_{vir}(M)$ as it is computed in our models. While $P(\nu(M)$ is determined by the merging history of each subhalo, $P(c(M))$ describes the scatter in concentration for haloes of equal mass (Bullock et al. 2001; Neto et al. 2007); therefore the two probabilities may be assumed independent. The single halo contribution to the total flux is given by

$$\Phi^{\rm cosmo}_{halo}(M,r,\nu,c) = \int\int_{\Delta\Omega} d\phi' d\theta' \int_{\rm l.o.s} d\lambda'$$

$$\left[\frac{\rho^2_\chi(M, r(\lambda,\lambda',\psi,\theta'\phi'),\nu,c)}{\lambda^2} J(x,y,z|\lambda',\theta'\phi')\right]. \qquad (18)$$

This equation is also used to derive the contribution of the smooth component of the MW itself.

Eq. 17 gives the average subhalo contribution to the Galactic annihilation flux within $\Delta\Omega$ along the direction ψ.

This contribution is shown in Fig. 5, together with the MW smooth halo component obtained with Eq.18, for the two models considered in this analysis, for $\Delta\Omega = 10^{-5}$ sr, corresponding to an experimental angular resolution of 0.1°. The sum of the MW smooth and clumpy diffuse contributions is shown as well. We define this sum as our "annihilation signal", which will be multiplied by Eq.16 to obtain the predicted γ-ray diffuse flux from neutralino annihilation in our Galaxy. In the small box we show a zoom at small angles of the annihilation signal and we superimpose the signal obtained in Pieri et al. (2007) for two similar models (we refer to their paper for the detailed explanation of models). Our models give a higher flux at the Galactic Center, where the signal is dominated by the MW smooth contribution. This is due to the different MW profile adopted. Yet, we find one order of magnitude of enhancement at the GC in the subdominant subhalo contribution as well, due to the presence of $P(\nu(M))$ in our determination of flux. Since more concentrated halos are closer to the GC in our approach, the enhancement is greater close to the GC: indeed, at the anticenter it goes down to a factor 2.

We have used the $P(\nu(M))$ for the ellipsoidal collapse in Eq. 17. We have checked that using the corresponding probability function for the spherical collapse does not change the result on Φ^{cosmo}. This is due to the fact that the main difference between the two models resides at small values of ν. A small ν gives low concentration parameter and its contribution to Eq. 18 is then depressed with respect to that of a haloes with a higher ν.

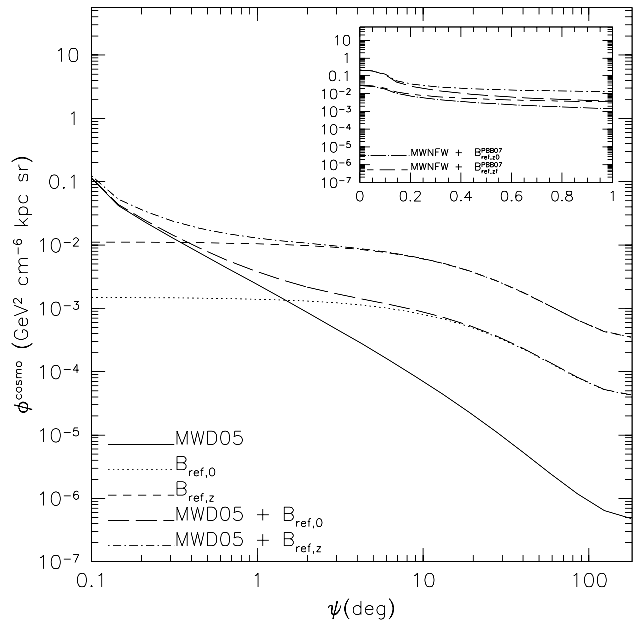

Figure 5. Subhalo contribution to the γ-ray flux for the two different models for the concentration parameters described in the text. MW smooth and clumpy contributions are shown separately, together with their sum. In the small box, zoomed at small angles from the Galactic Center only the sum is shown, and it is compared with the values obtained in Pieri et al. (2007).

4.3 Normalization to EGRET data

In order to make predictions on detectability, we impose the best value of Φ^{PP} compatible with the available experimental limits. As in Pieri et al. (2007), we first assume the optimistic model where $m_\chi = 40\ GeV$, $\sigma_{\rm ann}v = 3 \times 10^{-26}\ cm^3\ s^{-1}$ and the branching ratio is 100% in $b\bar{b}$. We then integrate Eq.16 above 3 GeV. This choice of parameters gives a value of $\Phi^{PP} = 2.6 \times 10^{-9}\,{\rm cm^4\,kpc^{-1}\,GeV^{-2}\,s^{-1}\,sr^{-1}}$.
We then compute the expected number of photons above 3 GeV in 1 year for a solid angle of 10^{-5} sr corresponding to the angular resolution of a GLAST-like satellite. The result for the $B_{ref,0}$ (dashed curve) and $B_{ref,z}$(dotted) models is shown in Fig. 6.

We compare the obtained number of events with the EGRET data for the diffuse Galactic component parametrized according to Bergström et al. (1998)

$$\frac{d\phi^{\rm gal-\gamma}_{\rm diffuse}}{d\Omega dE} = N_0(l,b)\ 10^{-6}\ E_\gamma^{-2.7}\,\frac{\gamma}{\rm cm^2\,s\,sr\,GeV}, \qquad (19)$$

and with the diffuse extragalactic γ emission, as extrapolated from EGRET data at lower energies (Sreekumar et al. 1998):

$$\frac{d\phi^{\rm extra-\gamma}_{\rm diffuse}}{d\Omega dE} = 1.38 \times 10^{-6} E^{-2.1}\,\frac{\gamma}{\rm cm^2\,s\,sr\,GeV}. \qquad (20)$$

The normalization factor N_0 in Eq. 19 depends only on

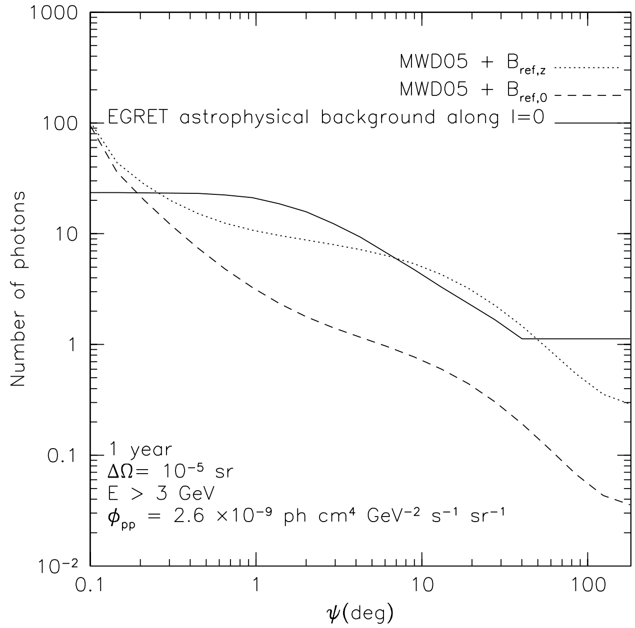

Figure 6. Number of photons above 3 GeV, in 1 year in a solid angle of 10^{-5} sr. The annihilation signal models $B_{ref,0}$ (dashed) and $B_{ref,z}$(dotted) are shown together with the EGRET diffuse expected Galactic and extragalactic background (solid), as a function of the angle of view ψ from the Galactic Center.

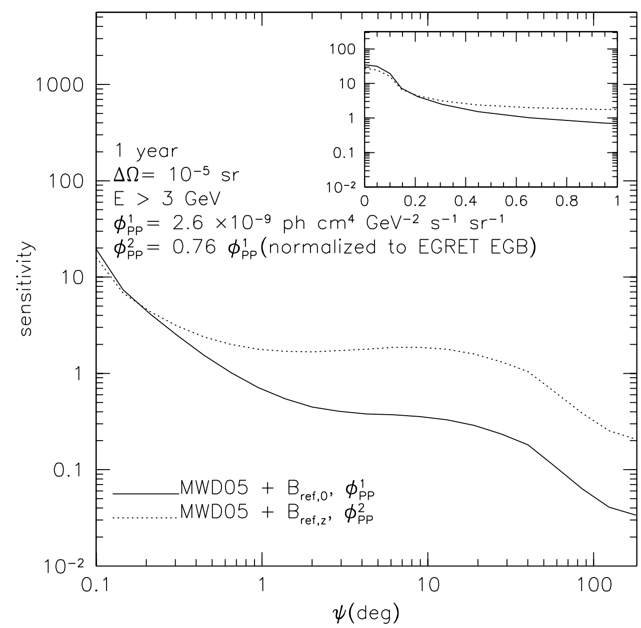

Figure 7. Sensitivity curves for a GLAST-like experiment, for the $B_{ref,0}$ (solid) and the $B_{ref,z}$(dotted) models described in the text. A zoom at small angles is provided in the superimposed frame.

the interstellar matter distribution. The resulting number of photons above 3 GeV in 1 year for $\Delta\Omega = 10^{-5}$ sr, computed along l=0 where its value is minimum, is shown in Fig. 6 (solid curve).

We find an excess of annihilation signal photons toward the Galactic centre in both models. Yet, the angular resolution of EGRET corresponding to $\Delta\Omega = 10^{-3}$ sr does not allow to reconstruct a spiky source as it is ours. We have checked that, if we compute the number of annihilation signal photons toward $\psi = 0$ smeared in a cone of view of 1°, it is below the number of EGRET detected photons for the same angular resolution.

Yet, the $B_{ref,z}$model exceeds the extragalactic diffuse measured background too, which is dominant above $\psi = 40°$. Since the extragalatic background is not due to any point source, we safely expect that it will scale with the solid angle. The number of annihilation signal photons produced in the $B_{ref,z}$model should then be less or at most comparable with the number of measured background photons. We make the optimistic assumption that the two numbers are comparable at $\psi = 40°$ where the discrepance is larger, and we thus fix $\Phi^{PP}_{B_{ref,z}} = 2.0 \times 10^{-9}\,\mathrm{cm^4\,kpc^{-1}\,GeV^{-2}\,s^{-1}\,sr^{-1}}$ for the $B_{ref,z}$model, correctly normalized to EGRET data, while we keep $\Phi^{PP}_{B_{ref,0}} = 2.6 \times 10^{-9}\,\mathrm{cm^4\,kpc^{-1}\,GeV^{-2}\,s^{-1}\,sr^{-1}}$ for the $B_{ref,0}$ model.

5 PROSPECTS FOR DETECTION

In this section we study the sensitivity of a GLAST-like apparatus for 1 year of effective data taking.

We define the experimental sensitivity σ as the ratio of the number n_γ of annihilation signal photons and the fluctuation of background events $n_{\rm bkg}$:

$$\begin{aligned} \sigma &\equiv \frac{n_\gamma}{\sqrt{n_{\rm bkg}}} \qquad (21) \\ &= \sqrt{T_\delta}\epsilon_{\Delta\Omega}\frac{\int A^{\rm eff}_\gamma(E,\theta_i)[d\phi^{\rm signal}_\gamma/dEd\Omega]dEd\Omega}{\sqrt{\int\sum_{\rm bkg}A^{\rm eff}_{\rm bkg}(E,\theta_i)[d\phi_{bkg}/dEd\Omega]dEd\Omega}} \end{aligned}$$

where $T_\delta = 1$ year is the effective observation time and ϕ_{bkg} is the background flux given by Eqs.19 and 20, computed along l=0, that we assume to be composed by astrophysical photons only. The quantity $\epsilon_{\Delta\Omega}$ is the fraction of signal events within the optimal solid angle $\Delta\Omega$ corresponding to the angular resolution of the instrument and it is optimistically set to 1. $A^{\rm eff}$ is the effective detection area defined as the detection efficiency times the geometrical detection area. We use $A^{\rm eff} = 10^4\,\mathrm{cm}^2$, independent from the energy E and the incidence angle θ_i. Finally we assume an angular resolution of 0.1° and an energy threshold of 3 GeV.

The resulting sensitivity curves as a function of the angle of view ψ are shown in Fig.7 for the $B_{ref,0}$ (solid curve) and $B_{ref,z}$(dotted) annihilation signal models. In the small box a zoom at GC is shown. An almost 2 σ around 10° is found for the $B_{ref,z}$model. The same model would be detected at about 30 σ at the Galactic Centre. As far as the $B_{ref,0}$ model is concerned, it would show up with $\sim 40\sigma$ effect toward the GC, that would rapidly fall down 1 σ after 0.5°. A 5 σ detection at the Galactic Center would be possible for both models with a value of Φ^{PP} even 6 times lower. In case of a striking excess detection along the GC, a milder excess a larger angles could be a hint for the discrimination about the models, though no discovery could be claimed.

Pieri et al. (2007) studied the detectability of resolved haloes which would shine above the Galactic foreground,

finding in their best case scenario that only a tenth of large mass haloes would be detected, with a mass slope of -2 for the halo mass function.

Repeating their analysis is beyond the goal of this paper. Yet we note that the effect of including the $P(\nu(M))$ factor in Eq. 17 with respect to the concentration models in Pieri et al. (2007) leads to an enhancement of the Galactic foreground. We thus expect that including $P(\nu(M))$ will be compensated by the increased foreground and we don't expect a dramatic change in the number of detectable haloes. As a further test, we have computed the sensitivity of a GLAST-like experiment for a $\mathrm{B}_{ref,z}$halo once Φ_{PP} has been normalized to the EGRET data. We chose the closer $M = 10^{-6} M_{\odot}$ halo, located at 9.5×10^{-2} pc from the sun. We chose $\nu = 2.4$ given from the probability of finding 1 halo with such a value in a 1 pc^3 sphere around the sun. We conservatively considered only the astrophysical background in Eq. 22, while the annihilation signal foreground should be considered too. Even in these very optimistic hypothesis, we found that the source would produce a 5 σ effect only furtherly multiplying by a factor of 4 the concentration parameter. This could be achieved using the lognormal probability $P(c(M))$ but with a ridicolously small probability.
We conclude that the effect of introducing the $P(\nu(M))$ can only be observed in a global enhancement of the diffuse Galactic annihilation foreground.

6 CONCLUSIONS

In this paper we have, for the first time, derived an analytical description of the mass function and distribution of rareness of density peaks in the subhalo population of our Galaxy, applying the extended Press & Schecter formalism. To make the calculation possible, tidal interactions and close encounters between subhaloes have been neglected. Very small (micro solar mass) subhaloes are extremely concentrated, therefore, at least for them, our approximation is a reasonable one.

The obtained results are valid over the whole range of subhalo masses $[10^{-6}, 10^{10}] M_{\odot}$ and thus confirm and extend the results of the N-body simulations, whose resolution is still far too low in order to simulate coherently this mass range.

Making use of the results of Diemand et al. (2005b) on the distribution of different σ-peak material inside our Galaxy, we have been able to shape and model the total expected annihilation γ-ray foreground, statistically taking into account the merging history of each progenitor.

We have used the best case particle physics scenario to derive predictions for the detectability of such a signal with a GLAST-like experiment. We have shown how both the merging history and the intrinsic properties of the halo formation can contribute to an enhancement of the expected flux, by arising the inner concentration of subhalos. Yet the real concentration of the single subhalo today remains an open question. We use two models which result in very different inner densities inside the haloes. In the first model we assume that the inner shells of the subhaloes remain frozen at the moment they enter the parent halo and thus compute the concentration parameter at the merging epoch, as it is derived in our calculations. Alternatively we assume that the subhaloes continue to evolve with redshift, and thus compute the halo properties today. We use the Bullock et al. (2001) model for the concentration parameter at $z = 0$, extrapolated at low masses. We refer to Pieri et al. (2007) for the effect of using different models.

Our results on detectability show that a detection would be possible and impressive toward the GC for both models. This detection would be mainly due to the spike in the MW halo at the GC. Unfortunately, a reliable modeling of the astrophysical background coming from the GC and of the effect of the central Super Massive Black Hole on the inner DM density profile are still poorly known.

A 2-σ effect would show up as well, around $\sim 10^{\circ}$ from the GC, only for the $\mathrm{B}_{ref,z}$model. Though no discovery could be claimed for, this could be a significant hint for the existence of such a population of subhaloes, and it would be propulsive for successive studies with upcoming experimental technologies.

A final note on the metodology. In the present work we derived the final subhalo mass function starting from all progenitor haloes at any redshift. We did so in order to directly compare our analytical results to the results obtained by Diemand et al. (2005b) using N-Body simulations. However, the subhalo population should indeed be derived starting from the population of "satellite haloes" directly accreted by the proto-halo (also called main progenitor) at all previous times (Tormen 1997), since only a fraction of progenitors at redshift z merge directly with the main halo progenitor. Unfortunately, the mass function of satellite haloes cannot be obtained analytically: it requires Monte Carlo simulations of the merging history tree of halo formation (Somerville & Kolatt 1999; van den Bosch 2002; van den Bosch et al. 2005). We are currently working on this issue (Giocoli et al, in prep.), and it will be interesting to compare the results obtained using the two methods.

REFERENCES

Aharonian, F. A., Hofmann, W., Konopelko, A. K., Völk, H. J. 1997, Astroparticle Physics, 6, 343
Appelquist, T., Cheng, H.-C., & Dobrescu, B. A. 2001, Physical Review D, 64, 035002
Astier, P., et al. 2006, A$A, 447, 31
Baixeras C. 2003, Nucl. Phys. Proc. Suppl., 114, 247
Berezinsky, V., Dokuchaev, V., & Eroshenko, Y. 2003, Physical Review D, 68, 103003
Bergström L., et al., 1998, Astroparticle Phys. 9, 137
Bergström L., 2000, Rept. Prog. Phys., 63, 793
Bertone G., Hoooper D. & Silk J., 2005, Phys. Rept., 405, 279
Bertone G. et al., 2005, Phys. Rev. D, 72, 103502
Bertone G., Merritt D., 2005, Mod. Phys. Lett., A20, 1021
Blasi P.,Sheth R. K., 2000 Phys. Lett. B, 486, 233
Bond, J. R., Cole, S., Efstathiou, G., & Kaiser, N. 1991, ApJ, 379, 440
Bullock J. et al., 2001, MNRAS, 321, 559
De Lucia, G., Kauffmann, G., Springel, V., White, S. D. M., Lanzoni, B., Stoehr, F., Tormen, G., & Yoshida, N. 2004, MNRAS, 348, 333
Diemand, J., Moore, B., & Stadel, J. 2004, MNRAS, 352, 535

Diemand J., Moore B., Stadel J., 2004, MMRAS, 353, 624
Diemand, J., Moore, B., & Stadel, J. 2005, NATURE, 433, 389
Diemand, J., Madau, P., & Moore, B. 2005, MNRAS, 364, 367
Diemand J., Kuhlen M., Madau P., 2006, Astrophys. J., 649, 1
Diemand J., Kuhlen M., Madau P., 2007, Astrophys. J., 657, 262
Diemand J., Kuhlen M., Madau P., 2007, astro-ph/0703337
Dimopoulos S., 1990, Phys. Lett. B, 246, 347
Eke, V. R., Cole, S., & Frenk, C. S. 1996, MNRAS, 282, 263
Fornengo N., Pieri L., Scopel S., 2004, Phys. Rev. D, 70, 103529
Gao, L., White, S. D. M., Jenkins, A., Stoehr, F., & Springel, V. 2004, MNRAS, 355, 819
Ghigna, S., Moore, B., Governato, F., Lake, G., Quinn, T., & Stadel, J. 1998, MNRAS, 300, 146
Ghigna, S., Moore, B., Governato, F., Lake, G., Quinn, T., & Stadel, J. 2000, Astrophys.J., 544, 616
Giocoli, C., Moreno, J., Sheth, R. K., & Tormen, G. 2007, MNRAS, 376, 977
Green, D. A., Tuffs, R. J., & Popescu, C. C. 2004, MNRAS, 355, 1315
Green, A. M., Hofmann, S., & Schwarz, D. J. 2005, Journal of Cosmology and Astro-Particle Physics, 8, 3
Hofmann, S., Schwarz, D. J., & Stöcker, H., 2001, Phys. Rev. D, 64, 083507
Jungman, G., Kamionkowski, M., & Griest, K. 1996, Phys. Rep., 267, 195
Koushiappas S. M., 2006, Phys. Rev. Lett. 97, 191301
Lacey, C., & Cole, S. 1993, MNRAS, 262, 627
Merritt, D., Milosavljević, M., Verde, L., & Jimenez, R., 2002, Phys. Rev. Lett., 88, 191301
Moore, B., Ghigna, S., Governato, F., Lake, G., Quinn, T., Stadel, J., & Tozzi, P., 1999, Astrophys. J. Lett., 524, L19
Morselli A. et al., 1997, in Proc. of the 32nd Rencontres de Moriond
Navarro, J. F., Frenk, C. S., & White, S. D. M., 1997, Astrophys. J., 490, 493
Navarro, J. F., Hayashi, E.; Power, C.; Jenkins, A. R.; Frenk, C. S. et al., 2004, MNRAS, 349, 1039
Neto, A. F., et al. 2007, ArXiv e-prints, 706, arXiv:0706.2919
Oda T., Totani T., Nagashima M., 2005, Astrophys. J., 633, L65
Pieri L., Branchini E., Hofmann S., 2005, Phys. Rev. Lett. 95, 211301
Pieri L., Bertone G., Branchini E., arXiv:0706.2101 (astro-ph)
Press, W. H., & Schechter, P. 1974, ApJ, 187, 425
Quinn, P. J., & Zurek, W. H. 1988, ApJ, 331, 1
Seljak, U., & Zaldarriaga, M. 1996, ApJ, 469, 437
Servant G., Tait T. M. P., 2003, Nucl. Phys. B, 650, 391
Sheth, R. K. 2003, MNRAS, 345, 1200
Sheth, R. K., Mo, H. J., & Tormen, G. 2001, MNRAS, 323, 1
Sheth, R. K., & Tormen, G. 2002, MNRAS, 329, 61
Somerville, R. S., & Kolatt, T. S. 1999, MNRAS, 305, 1
Spergel D. N., et al., 2003, Astrophys. J. Suppl. 148, 175.
Sreekumar P. et al., 1998, ApJ ,494, 523
Springel, V., et al. 2005, NATURE, 435, 629
Stoehr F., et al., 2003, MNRAS, 345, 1313
Tegmark, M., et al. 2006, Phys. Rev. D, 74, 123507
Tormen, G. 1997, MNRAS, 290, 411
Tormen, G., Moscardini, L., & Yoshida, N. 2004, MNRAS, 350, 1397
Ullio P., H. Zhao H., Kamionkowski M., 2001, Phys. Rev. D, 64, 043504
van den Bosch, F. C. 2002, MNRAS, 331, 98
van den Bosch, F. C., Tormen, G., & Giocoli, C. 2005, MNRAS, 359, 1029
Weekes T. C. et al., 1997, in Proc. of the 25th ICRC, 5, 173
Zaroubi, S., Naim, A., & Hoffman, Y. 1996, ApJ, 457, 50